

Application of Nonlinear Monotone Finite Volume Schemes to Advection-Diffusion Problems

Yuri Vassilevski, Alexander Danilov, Ivan Kapyrin, and Kirill Nikitin

Abstract Two conservative schemes for the nonstationary advection-diffusion equation featuring nonlinear monotone finite volume methods (FVMON) are considered. The first one is an operator-splitting scheme which uses discontinuous finite elements for the advection operator discretization and FVMON for the diffusion operator. The second one introduces another type of FVMON and is implicit second-order BDF in time. A brief description of the schemes and their properties is given. A numerical study is conducted in order to check their convergence and to compare them with conventional methods.

Keywords Monotone finite volumes, advection-diffusion.

MSC2010:65M08

1 Formulation of the methods

1.1 Model Problem

Let Ω be a bounded polyhedral domain in \mathbb{R}^3 with a boundary $\partial\Omega$. Consider the following model advection-diffusion problem (for simplicity, with homogeneous Dirichlet boundary conditions):

Yuri Vassilevski, Alexander Danilov, Ivan Kapyrin, and Kirill Nikitin
Institute of Numerical Mathematics RAS, 8 Gubkina, Moscow 119333, Russia, e-mail:
vasilevs@dodo.inm.ras.ru, danilov@dodo.inm.ras.ru, kapyrin@dodo.inm.ras.ru, nikitink@dodo.inm.ras.ru

$$\frac{\partial C}{\partial t} - \nabla \cdot D \nabla C + \mathbf{b} \cdot \nabla C = F \quad \text{in } \Omega \times (0, T], \quad (1a)$$

$$C = 0 \quad \text{on } \partial\Omega \times (0, T], \quad (1b)$$

$$C = C_0(x) \text{ in } \Omega \text{ at } t = 0. \quad (1c)$$

Here, C is the contaminant concentration, $\mathbf{b} = \mathbf{b}(x)$ is a conservative convective flux field, $F = F(x)$ is the function of sources or sinks, and $D = D(x)$ is a symmetric positive definite 3×3 diffusion tensor.

1.2 Operator-splitting scheme: DFEM+FVMON

The operator-splitting scheme is designed for tetrahedral grids. It is explained in details in [9], here we give only a brief description. Let a conformal tetrahedral mesh ε_h be introduced in the computational domain Ω . Denote the mesh cells by E_i , $i = 1, \dots, N_E$, the nodes by $O_i = (x_i, y_i, z_i)$, $i = 1, \dots, N_P$. We define the space of discontinuous piecewise linear functions on ε_h

$$W_h = \{v \in L_2(\Omega), v|_E \in P_1(E), v|_{\partial E \cap \partial\Omega} = 0 \forall E \in \varepsilon_h\}.$$

The concentration is approximated by piecewise linear discontinuous functions from W_h . The scheme involves splitting over physical components, and the diffusion and convection operators are handled at different substeps. More specifically, at each substep, we solve the incomplete equation (see [8]). The time step of the scheme is defined as follows:

$$I. \int_E \frac{C_h^{n+\frac{1}{2}} - C_h^n}{\Delta t/2} w_h dx - \int_E \mathbf{b} C_h^n \cdot \nabla w_h dx + \int_{\partial E} \mathbf{b} C_{h,in}^n \cdot \mathbf{n} w_h ds = \int_E F^n w_h dx$$

$$\forall w_h \in W_h(E), \quad \forall E \in \varepsilon_h, \quad (2a)$$

$$II. \int_E \frac{C_h^{*,ad} - C_h^n}{\Delta t} w_h dx - \int_E \mathbf{b} C_h^{n+\frac{1}{2}} \cdot \nabla w_h dx + \int_{\partial E} \mathbf{b} C_{h,in/out}^{n+\frac{1}{2}} \cdot \mathbf{n} w_h ds =$$

$$= \int_E F^{n+\frac{1}{2}} w_h dx \quad \forall w_h \in W_h(E), \quad \forall E \in \varepsilon_h, \quad (2b)$$

$$III. \text{ Slope limiter: } C_h^{*,ad} \longrightarrow C_h^{n+1,ad},$$

$$IV. \int_E \frac{\bar{C}_{h,E}^{n+1} - \bar{C}_{h,E}^{n+1,ad}}{\Delta t} dx = - \sum_{i=1}^4 r_{E,i}^{n+1} = - \int_{\partial E} \mathbf{r}_E^{n+1} \cdot \mathbf{n} ds \quad \forall E \in \varepsilon_h, \quad (2c)$$

$$V. C_h^{n+1} = C_h^{n+1,ad} + (\bar{C}_h^{n+1} - \bar{C}_h^{n+1,ad}). \quad (2d)$$

The convection operator is approximated by an explicit predictor-corrector scheme with an upwind regularization in the corrector. The intermediate concentration $C_h^{n+\frac{1}{2}}$ is calculated in predictor (2a), while $C_h^{*,ad}$ in the corrector is calculated from the convective fluxes at the intermediate time level. In the integral over the boundary, $C_{h,in/out}^{n+\frac{1}{2}}$ is taken on the tetrahedron lying upstream. The slope-limiting procedure (2c) is applied to $C_h^{*,ad}$. Next, implicit scheme (2d) is used to calculate the addition to the mean concentration, \bar{C}_h due to the diffusive fluxes $r_{E,i}^{n+1}$ through the i -th faces of E . The values of \bar{C}_h^{n+1} and $r_{E,i}^{n+1}$ are determined by the nonlinear monotone finite-volume method (FVMON) [3]. Its goal is to derive an as sparse as possible monotone approximation matrix by forming two-point diffusive flux approximations. Then, the solution \bar{C}_h^{n+1} remains nonnegative for nonnegative $\bar{C}_h^{n+1,ad}$. The idea of the two-dimensional FVMON for diffusion problems was set forth in [4]. The details of the present scheme formulation can be found in [9]. The main idea of the scheme construction is based on the following steps:

1. Define the collocation points bearing the degrees of freedom inside each tetrahedron. For cell E we define the point X_E .
2. For two neighbouring tetrahedra E_+, E_- and the corresponding degrees of freedom C_{X_+}, C_{X_-} we define the diffusion flux through the common face e :

$$\mathbf{r}_e \cdot \mathbf{n}_e = K_+(\mathbf{C}_X)C_{X_+} - K_-(\mathbf{C}_X)C_{X_-}. \tag{3}$$

Here \mathbf{C}_X is the global vector of unknowns, \mathbf{n}_e is the normal vector to face e . The flux defined in (3) has a two-point approximation stencil with coefficients $K_+(\mathbf{C}_X), K_-(\mathbf{C}_X)$ depending on the vector of unknown concentrations. The algorithm of their calculation guarantees positivity of coefficients in case of non-negative vector \mathbf{C}_X .

3. Assemble the global nonlinear system and solve it.

To implement step (2c), we find the projection \hat{c} of the solution $C_h^{n+1,ad}$ onto the set \mathbb{B} of the collocation points in cells and solve the FVMON problem for the desired concentrations \hat{c}^{diff} at the points of \mathbb{B} :

$$(\mathbf{V} + \mathbf{A}(\hat{c}^{diff})\Delta t) \hat{c}^{diff} = \mathbf{V}\hat{c}. \tag{4}$$

Here, \mathbf{V} is a diagonal matrix of element volumes and $\mathbf{A}(\hat{c}^{diff})$ is an asymmetric matrix whose elements depend on \hat{c}^{diff} . All the off-diagonal and diagonal nonzero elements of $\mathbf{A}(\hat{c}^{diff})$ are negative and positive, respectively, for nonnegative \hat{c}^{diff} . Moreover, the transpose $(\mathbf{A}(\hat{c}^{diff}))^T$ is row diagonally dominant. Therefore, $(\mathbf{A}(\hat{c}^{diff}))^T$ is an M-matrix and $[(\mathbf{A}(\hat{c}^{diff}))^T]^{-1}_{ij} \geq 0$. Since $(\mathbf{A}^{-1})^T = (\mathbf{A}^T)^{-1}$, the matrix $\mathbf{A}(\hat{c}^{diff})$ is monotone. Nonlinear system (4) is solved by the Picard iteration algorithm

$$(\mathbf{V} + \mathbf{A}(\hat{c}^{diff,k})\Delta t) \hat{c}^{diff,k+1} = \mathbf{V}\hat{c}$$

with the initial approximation $\hat{c}^{diff,0} = \hat{c} \geq 0$. Since the matrix $\mathbf{V} + \mathbf{A}(\hat{c}^{diff,k})\Delta t$ is monotone for any nonnegative $\hat{c}^{diff,k}$, all the iterative approximations $\hat{c}^{diff,k+1}$ are nonnegative as well; i.e., scheme (4) is monotone.

After \hat{c}^{diff} is determined, we use the formula

$$\bar{C}_{h,E}^{n+1} - \bar{C}_{h,E}^{n+1,ad} = \hat{c}_E^{diff} - \hat{c}_E \quad \forall E \in \mathcal{E}_h$$

and find the addition to the mean concentrations due to diffusive fluxes, as required in (2e).

1.3 Implicit FVMON scheme

The idea of the implicit nonlinear monotone finite volume scheme is to derive a discretization for the total advective-diffusive flux $\mathbf{r} = -D\nabla C + C\mathbf{b}$ and use the implicit second-order BDF discretization in time. The method is applicable to arbitrary conformal meshes with polyhedral cells and jumping full anisotropic diffusion tensors as well as variable convection fields.

For each cell E , we assign one degree of freedom, C_E , for concentration C . If two cells E_+ and E_- have a common face f and the normal \mathbf{n}_f is exterior to E_+ , the two-point flux approximation is as follows:

$$\mathbf{r}_f \cdot \mathbf{n}_f = M_f^+ C_{E_+} - M_f^- C_{E_-}, \tag{5}$$

where M_f^+ and M_f^- are some coefficients. In a linear FV method, these coefficients are equal and fixed. In the nonlinear FV method, they may be different and depend on concentrations in surrounding cells.

Diffusive flux $\mathbf{r}_d = -D\nabla C$ is discretized using the nonlinear two-point flux approximation [1, 5] with non-negative coefficients $K_f^\pm(C) \geq 0$:

$$(-D\nabla C)_f \cdot \mathbf{n}_f = K_f^+(C)C_{T_+} - K_f^-(C)C_{T_-}. \tag{6}$$

Advective flux $\mathbf{r}_a = C\mathbf{b}$ is approximated via an upwinded linear reconstruction \mathcal{R}_T of the concentration over cell T [6, 7]:

$$\mathbf{r}_{f,a} \cdot \mathbf{n}_f = b_f^+ \mathcal{R}_{E_+}(\mathbf{x}_f) + b_f^- \mathcal{R}_{E_-}(\mathbf{x}_f), \tag{7}$$

where

$$b_f^+ = \frac{1}{2}(b_f + |b_f|), \quad b_f^- = \frac{1}{2}(b_f - |b_f|), \quad b_f = \frac{1}{|f|} \int_f \mathbf{b} \cdot \mathbf{n}_f \, ds.$$

We define the reconstruction \mathcal{R}_E as a linear function

$$\mathcal{R}_E(\mathbf{x}) = C_E + \mathbf{g}_E \cdot (\mathbf{x} - \mathbf{x}_E), \quad \forall \mathbf{x} \in E, \tag{8}$$

with a gradient vector \mathbf{g}_E . Since C_E is collocated at the barycenter of E , this reconstruction preserves the mean value of the concentration for any choice of \mathbf{g}_E .

The gradient vector \mathbf{g}_E is the solution to the following constrained minimization problem:

$$\mathbf{g}_E = \arg \min_{\tilde{\mathbf{g}}_E \in \mathcal{G}_E} \mathcal{J}_E(\tilde{\mathbf{g}}_E), \tag{9}$$

where the functional

$$\mathcal{J}_E(\tilde{\mathbf{g}}_E) = \frac{1}{2} \sum_{\mathbf{x}_k \in \Sigma_E} [C_E + \tilde{\mathbf{g}}_E \cdot (\mathbf{x}_k - \mathbf{x}_E) - C_k]^2$$

measures deviation of the reconstructed function from the targeted values C_k collocated at points \mathbf{x}_k from a set Σ_E of the neighbouring collocation points.

The set of admissible gradients \mathcal{G}_E is defined via three constraints suppressing non-physical oscillations (see [7] for more details).

As the result, we represent the advective flux as the sum of a linear part (the first-order approximation) and a nonlinear part (the second-order correction):

$$\mathbf{r}_{f,a} \cdot \mathbf{n}_f = A_f^+(C)C_+ - A_f^-(C)C_-, \tag{10}$$

where

$$A_f^\pm(C) = \pm b_f^\pm (1 + \mathbf{g}_\pm \cdot (\mathbf{x}_f - \mathbf{x}_\pm) C_\pm^{-1}) \geq 0, \tag{11}$$

subscript \pm stands for E_\pm and $\mathbf{g}_\pm = \mathbf{g}_{E_\pm}$.

The resulting nonlinear system is solved using the Picard iterations method. The matrix is monotone on each iteration (see [7]) providing a nonnegative solution.

2 Results of numerical experiments

2.1 Smooth analytical solution

In the first test case the computational domain Ω is a unit cube $[0; 1]^3$, the advection field $\mathbf{b} = (0.1; z/10; y/10)$. Two diffusion tensors and the corresponding analytical solutions are considered:

1. $D = I, \quad C(x, y, z, t) = (1 - x^2) \sin(y) e^{-z} \sin(t)$
2. $D = 10^{-5} I \quad C(x, y, z, t) = x^2 \sin(y) e^{-z} \sin(t)$

The first test case features dominating diffusion, the second - dominating advection. The choice of analytical solutions is explained by the desire to obtain nonnegative right-hand sides in the discretization of Eq. (1) in order to verify the monotonicity of the schemes. Recall that only the FVMON guarantees the absence of negative concentrations in this case (although it is unsuitable for problems admitting negative concentrations). Three uniform structured tetrahedral meshes were used in the

Table 1 Solution and flux L_2 -errors for DFEM+FVMON scheme

Mesh	case $D = I$		case $D = 10^{-5}I$	
	e_C	e_r	e_C	e_r
1	$1.4 \cdot 10^{-3}$	$2.8 \cdot 10^{-2}$	$4 \cdot 10^{-4}$	$3.8 \cdot 10^{-7}$
2	$4 \cdot 10^{-4}$	$1.3 \cdot 10^{-2}$	$1 \cdot 10^{-4}$	$1.8 \cdot 10^{-7}$
3	$1.2 \cdot 10^{-4}$	$6 \cdot 10^{-3}$	$2.5 \cdot 10^{-5}$	$8.3 \cdot 10^{-8}$

Table 2 Solution L_2 -error (e_C) for the BDF FVMON scheme

Mesh	case $D = I$	case $D = 10^{-5}I$
1	$2.2 \cdot 10^{-3}$	$5.3 \cdot 10^{-3}$
2	$5.7 \cdot 10^{-4}$	$1.5 \cdot 10^{-3}$
3	$1.4 \cdot 10^{-4}$	$4.0 \cdot 10^{-4}$

computations. The coarsest of them consisted of 3072 tetrahedra (mesh 1). The other two were obtained by uniformly refining the first and contained 24 576 (mesh 2) and 196 608 (mesh 3) elements, respectively (the mesh size was halved in each refinement procedure). In all the schemes, the time steps used in the tests were 0.025 for mesh 1, 0.0125 for mesh 2, and 0.00625 for mesh 3. The errors were calculated for the solution at the time $T = 1$ and can be seen in tables 1 and 2.

For both schemes we calculate the discrete L_2 -error for the solution e_C . For the splitting scheme the diffusion flux L_2 -error e_r is computed as well (not implemented yet for the implicit scheme). In both cases we observe second order convergence for the solution, the splitting scheme shows first order convergence for the diffusion fluxes.

2.2 Sharp front resolution

Consider the front of concentration propagating from a constant source occupying a section on the boundary of the domain $\Omega = (0; 1) \times (-0.5; 0.5) \times (-0.5; 0.5)$. More specifically, the following inhomogeneous boundary conditions are set at $x = 0$:

$$C(0, y, z) = \begin{cases} 1 & \text{if } |y| < \frac{1}{4}, |z| < \frac{1}{4}, \\ 0 & \text{elsewhere.} \end{cases}$$

The initial concentration is zero in the entire domain Ω , and the convective flux is $\mathbf{b} = (1, 0, 0)$. For the solution to have a sharp front, the diffusion tensor is chosen to be small with respect to convection: $D = 10^{-4}I$.

The analytical solution to this problem in the half-space $x \geq 0$ was found in [2]. Passing to the bounded domain Ω , we set Dirichlet conditions on all its boundaries. A non-uniform tetrahedral grid is used for the domain discretization. The numerical solutions are compared with the analytical one at the time $T = 0.5$ and with the

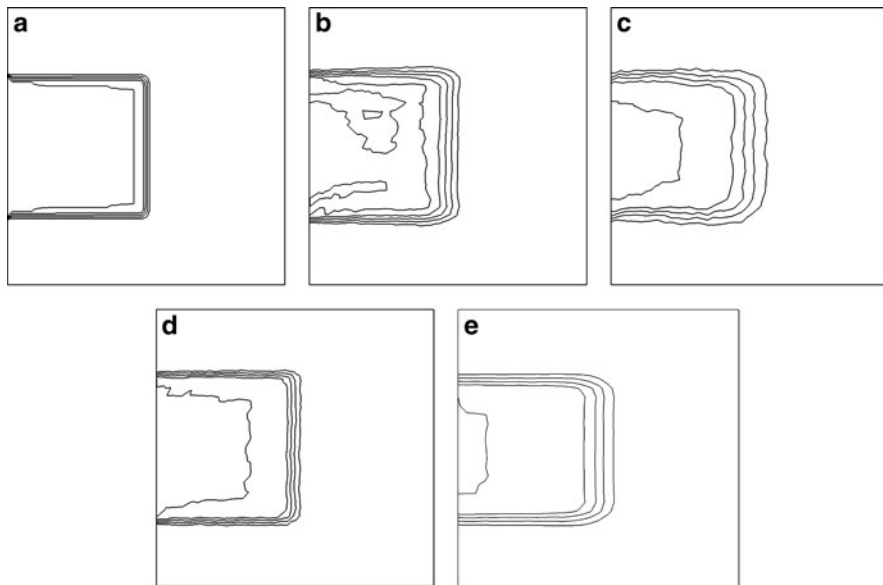


Fig. 1 Analytical and numerical solutions of the front propagation problem: a—analytical; b—implicit BDF P_1 -FEM with SUPG; c— BDF implicit HMFEM scheme; d— operator-splitting scheme DFEM+FVMON; e— BDF implicit FVMON scheme.

Table 3 Minima of mean cell concentrations

P_1 -FEM	MFEM	DFEM+FVMON	impl. FVMON
$-1.8 \cdot 10^{-1}$	$-6.4 \cdot 10^{-2}$	0	0

solutions obtained by conventional methods: BDF implicit schemes of P_1 -FEM with SUPG and HMFEM with upwinding.

Figure 1 displays the exact (a) and approximate (b-e) solutions at $T = 0.5$ in the plane $y = 0$. The contour lines correspond to the concentration values 0.2, 0.4, 0.6, 0.8, and 1. The conventional methods are nonmonotone, so the solution takes negative values (Table 3), whereas the considered monotone schemes guarantee non-negativity of the solution. Figure 1b shows that FEM with SUPG exhibits strong oscillations. Since the FEM is strongly dispersive, a concentration contour line corresponding to 1 appears in Fig.1b in the area where the solution must be the identical unit. Hybrid MFEM demonstrates high numerical dissipation in Fig.1c. The operator-splitting scheme shows the lowest numerical diffusion (rf.Fig.1d). The implicit FVMON scheme exhibits numerical diffusion comparable to that of FEM with SUPG method.

Conclusions

The two schemes featuring the nonlinear monotone finite volumes prove to be a good alternative to conventional methods especially in cases when monotonicity (in the sense of non-negative concentrations) is important. The operator-splitting scheme makes use of discontinuous finite elements applied for the advection operator discretization. It produces low numerical diffusion. In this scheme diffusion is treated implicitly, and advection explicitly. Thus the time step of the scheme depends on the CFL number. An efficient solution to accelerate its performance is to use different time steps for advection and diffusion. The extra computational burden due to nonlinearity seems to be admissible: the scheme is approximately 20% slower than a linear similar splitting scheme [9].

The BDF implicit scheme of FVMON also shows second order convergence on analytical solutions both for advection and diffusion dominated problems. While suffering from higher numerical diffusion, the scheme has no time step restriction and thus can be more suitable in terms of computational efficiency. Also the scheme is applicable to arbitrary polyhedral cells. Both schemes guarantee non-negativity of the solution in case of non-negative source terms and proper boundary conditions.

Acknowledgements This work has been supported in part by RFBR grants 09-01-00115-a, 11-01-00971-a and the federal program “Scientific and scientific-pedagogical personnel of innovative Russia”

References

1. Danilov A., Vassilevski Yu. A monotone nonlinear finite volume method for diffusion equations on conformal polyhedral meshes. *Russian J. Numer. Anal. Math. Modelling*, No.24, pp.207–227, 2009.
2. Feike J.L., Dane J.H. Analytical solutions of the one-dimensional advection equation and two- or three-dimensional dispersion equation. *Water Resources Research*, vol.26, No.7, pp.1475–1482, 1990.
3. Kapyrin I.V. A Family of Monotone Methods for the Numerical Solution of Three-Dimensional Diffusion Problems on Unstructured Tetrahedral Meshes. *Doklady Mathematics*, Vol. 76, No. 2, pp. 734–738, 2007.
4. Le Potier C. Schema volumes finis monotone pour des operateurs de diffusion fortement anisotropes sur des maillages de triangle non structures. *C.R.Acad. Sci. Paris*, Ser. I 341, pp.787–792, 2005.
5. Lipnikov K., Svyatskiy D., Vassilevski Yu. Interpolation-free monotone finite volume method for diffusion equations on polygonal meshes. *J. Comp. Phys.* Vol.228, No.3, pp.703–716, 2009.
6. Lipnikov K., Svyatskiy D., Vassilevski Yu. A monotone finite volume method for advection-diffusion equations on unstructured polygonal meshes. *J. Comp. Phys.* Vol.229, pp.4017–4032, 2010.
7. Nikitin K., Vassilevski Yu. A monotone nonlinear finite volume method for advection-diffusion equations on unstructured polyhedral meshes in 3D. *Russian J. Numer. Anal. Math. Modelling*, Vol.25, pp.335–358, 2010.

8. Siegel P., Mose R., Ackerer Ph. and Jaffre J. Solution of the advection-diffusion equation using a combination of discontinuous and mixed finite elements. *International Journal for Numerical Methods in Fluids*, Vol.24, p.595–613, 1997.
9. Vassilevski Yu.V., Kapyrin I.V. Two Splitting Schemes for Nonstationary Convection-Diffusion Problems on Tetrahedral Meshes. *Computational Mathematics and Mathematical Physics*, Vol.48, No. 8, pp. 1349-1366, 2008.

The paper is in final form and no similar paper has been or is being submitted elsewhere.